Composites Science and Technology 198 (2020) 108327

Contents lists available at ScienceDirect

Composites Science and Technology

journal homepage: http://www.elsevier.com/locate/compscitech

Plastic to elastic: Fungi-derived composite nanopapers with tunable tensile properties

Wan M.F.W. Nawawi [a,b,c], Mitchell P. Jones [a,d], Eero Kontturi [e], Andreas Mautner [a,**], Alexander Bismarck [a,b,f,*]

[a] Institute of Material Chemistry and Research, Polymer and Composite Engineering (PaCE) Group, Faculty of Chemistry, University of Vienna, Währinger Straße 42, 1090, Vienna, Austria
[b] Department of Chemical Engineering, Imperial College London, South Kensington Campus, London, SW7 2AZ, UK
[c] Department of Biotechnology Engineering, International Islamic University Malaysia, P.O. Box 10, 50728, Kuala Lumpur, Malaysia
[d] School of Engineering, RMIT University, Bundoora East Campus, PO Box 71, Bundoora, 3083, VIC, Australia
[e] Department of Bioproducts and Biosystems (BIO^2), School of Chemical Engineering, Aalto University, PO Box 16300, FI-00076, Aalto, Finland
[f] Department of Mechanical Engineering, Faculty of Engineering and the Built Environment, University of Johannesburg, South Africa

ARTICLE INFO

Keywords:
A. Fibres
A. Hybrid composites
B. Mechanical properties
Fungal chitin-β-glucan

ABSTRACT

Fungal chitin is attracting commercial and academic interest as a cheap, renewable, easily isolated and abundant alternative to crustacean chitin. Being covalently decorated with β-glucan, fungal chitin exhibits a native nanocomposite architecture that varies in fibre diameter and chitin to β-glucan ratio from species to species, resulting in mechanical properties ranging from brittle, high tensile strength, plastic-like properties to very tough and elastomeric rubber-like tensile properties if processed into paper form. This study utilised a mild alkaline process to extract chitin-β-glucan complexes from tree bracket fungi (*D. confragosa*) and common mushrooms (*A. bisporus*), which were then combined in varying ratios and hot pressed to form engineered composite nanopapers with tunable tensile properties. Fruiting bodies of common mushrooms, with almost proportional contents of chitin and β-glucan, exhibited a nanofibrous architecture resulting in very high tensile strengths, far outperforming crustacean-derived chitin. These nanopapers could then be plasticised in a controlled fashion through addition of extract from tree bracket fungi, which contains large quantities of β-glucan, to produce composite nanopapers. The fungal chitin extracts were significantly more hydrophobic than crustacean chitin, suggesting potential as a coating agent for hydrophilic materials, such as cellulose. These remarkable and controllable characteristics make fungi-derived materials versatile for a wide range of applications, including coatings, membranes, packaging and paper.

1. Introduction

Fungi have always played a critical role in many aspects of everyday life, from antibiotic medicines, to food products, such as beer, wine, bread, soy sauce, tempeh and meat substitutes, such as Quorn™. However, recent academic and commercial interest in fungi is increasingly focused towards the remarkable potential of fungal structural polymers, such as chitin, to produce composites and nanomaterials [1–4]. Chitin is a linear macromolecule composed of N-acetylglucosamine repeating units that is also the main component of the exoskeleton of most insects and other arthropods [5]. Chitin forms strong nanofibrils with a tensile strength in the range of ~1.6–3.0 GPa [6] due to hydrogen bonding along the chains, which give them rigidity [7]. Chitin extracted from fungi, offers a cheap, renewable, easily isolated and abundant alternative to more expensive, seasonally and regionally limited crustacean chitin [8–10].

Crustacean chitin normally has minimal residual proteins and is associated with sclerotized proteins and minerals, whereas fungal chitin is bound with other polysaccharides, such as glucan, which can occur in quantities exceeding the chitin content itself [11]. The lower purity of fungal chitin-β-glucan complexes has resulted in fungi generally being overlooked in materials science, with purer crustacean chitin

* Corresponding author. Institute of Material Chemistry and Research, Polymer and Composite Engineering (PaCE) Group, Faculty of Chemistry, University of Vienna, Währinger Straße 42, 1090, Vienna, Austria.
** Corresponding author.
E-mail addresses: andreas.mautner@univie.ac.at (A. Mautner), alexander.bismarck@univie.ac.at (A. Bismarck).

https://doi.org/10.1016/j.compscitech.2020.108327
Received 19 April 2020; Received in revised form 25 June 2020; Accepted 27 June 2020
Available online 30 June 2020

historically being preferred to produce chitinous biomedical and nanomaterials [8,12]. Strong alkaline treatments are sometimes used to remove fungal β-glucan from the chitin [13]. However, recent studies have proven that the pliable branched β-glucan associated with fungal chitin can be highly beneficial to the mechanical properties of fungal nanomaterials, acting as matrix thus providing a native nanocomposite architecture in nanopaper form that is both strong and tough [14]. Consequently, the significant and natural variations in chitin to β-glucan ratio and fibril dimensions in fungi can be utilised to produce both more brittle, high tensile strength, plastic-like nanofibre networks as well as very tough and elastomeric (rubber-like) networks exhibiting significant fibril pull-out at failure. Mechanical properties between these extremes can also be facilitated by combining fungal polymer extracts derived from different species.

This study aimed to produce composite nanopapers from common white button mushroom (*A. bisporus*) and tree bracket fungal fruiting body (*D. confragosa*) derived fungal chitin-β-glucan. Complexes of chitin and β-glucan were extracted from the fungal fruiting bodies using a mild alkaline treatment and combined in varying ratios to produce composite nanopapers with tunable mechanical performance, ranging from brittle, plastic-like properties to very tough and elastomeric rubber-like tensile properties, utilising the natural variations in fibril diameter and chitin to β-glucan ratio of these two species. The morphology, composition and molecular structure of the nanopapers were then analysed in addition to their physical, mechanical and surface properties.

2. Experimental section

2.1. Materials

Commercial chitin references derived from shrimp were purchased from Sigma-Aldrich (C9213, practical grade) as a primary reference for chemical analysis. Crab carapaces (*Cancer pagurus*, C-Quest Ltd., Dorset, UK) were used as a secondary source of crustacean chitin and finely ground in a ball mill prior to extraction and processing into crustacean-derived reference nanopapers. Common white button mushrooms (*Agaricus bisporus*) were purchased from a local store. Tree bracket fungi (*Daedaleopsis confragosa*), a polypore fungus commonly found on decaying willow trees, were collected from Wormwood Scrubs, London, UK (Google Earth location: 51° 31′ 13.57″ N, 0° 14′ 00.10″ W) during autumn. NaOH (Sigma Aldrich, pellets), HCl (Sigma-Aldrich, 37% w/w) and H_2SO_4 (Merck, 72% w/w) were used during chitin extraction and sugar hydrolysis. Sugar recovery standards (SRS) for carbohydrate analysis were prepared from L-(+)-arabinose (Calbiochem), D-(+)-galactose (Merck), D-(+)-glucosamine hydrochloride (Sigma-Aldrich), D-(+)-glucose (BDH Prolabo), D-(+)-mannose (Merck), L-(+)-rhamnose (BDH Prolabo) and D-(+)-xylose (Merck). All test liquids for inverse gas chromatography (iGC) were HPLC grade and purchased from Sigma-Aldrich: n-hexane, n-heptane, n-octane, n-nonane, n-decane, dichloromethane, ethyl acetate, acetone and acetonitrile. Ultrapure water (CENTRA-R 200 or PURELAB Classic, 18.2 MΩ cm^{-1} resistivity, <10 ppb inorganic impurities) was used for all experiments.

2.2. Chitin-β-glucan complex extraction from mushrooms and tree bracket fungi

A. bisporus mushrooms (500 g) were soaked in 1 L distilled water for 5 min and rinsed thrice to remove impurities before being blended for 5 min in a kitchen blender (Breville VBL065 Pro 800W, Oldham, UK) prior to extraction. *D. confragosa* tree brackets were soaked in water overnight before being diced into pieces (~5 mm × 5 mm × 5 mm) and blended for 10 min under the same conditions to achieve a fibrous slurry [15,16]. Water was then added to each respective slurry to achieve a volume of 1.5 L before being heated to 85 °C and stirred for 30 min. The suspensions were then cooled to 25 °C and centrifuged at 7000 rpm for 15 min at 18 °C. The resultant residue was resuspended in 1 M NaOH solution for 3 h at 65 °C. The suspension was cooled to 25 °C and then neutralised (pH 7) by repeated centrifugation and redispersion of the residue in water. The neutralised cake was then resuspended in water (0.8% w/v) and dispersed by blending for 1 min. The suspension was stored at 4 °C until further use.

2.3. Crustacean chitin extraction from crab shells

C. pagurus crab carapaces were treated using the same mild alkaline treatment described above with the exception that a demineralisation step had to be conducted between the heating of the suspension in water and NaOH [17] (Fig. 1). The centrifuged cake was demineralised by suspension in 1.5 L of 1 M HCl, which was stirred for 30 min. Following demineralisation, the suspension was cooled to 25 °C and then neutralised (pH 7) by repeated centrifugation and redispersion of the residue in water. The same alkaline treatment and storage conditions used for the fungal samples were then applied to the crustacean material.

2.4. Preparation of the neat chitinous nanopapers

Suspensions of *C. pagurus* (crab), *A. bisporus* (common mushroom) and *D. confragosa* (bracket fungus) with a consistency of 0.8% (w/v) were prepared for production of nanopapers with a grammage of 80 g/m^2. Nanopapers were produced by vacuum filtering this suspension over a filter paper (VWR 125 mm qualitative filter paper 413, particle retention 5–13 μm). The filter cake was peeled off the filter and wet pressed twice between blotting papers (3 MM CHR blotting paper, VWR) to remove excess moisture, changing the blotting paper in-between pressing steps. Extracts were then dried under a 5 kg mass in an oven at 120 °C for 3 h and left overnight under the mass at room temperature.

2.5. Preparation of composite chitinous nanopapers

Composite nanopapers were prepared by blending *A. bisporus* (0.8% w/v) and *D. confragosa* (1.0% w/v) extracts in ratios of 25:75, 50:50 and 75:25 wt.%. Stock suspensions were diluted through the addition of 100 mL of water prior to vigorous mixing by hand for several seconds. Nanopapers with a grammage of 80 g/m^2 were then prepared using the same procedure for neat nanopapers outlined above.

2.6. Morphology and chemical composition of (composite) nanopapers

Scanning Electron Microscopy (SEM) imaging of each nanopaper was performed using a LEO Gemini 1525 FEG-SEM (Oberkochen, Germany). An accelerating voltage of 5 kV was used. Samples were air dried and chromium coated (K550 sputter coater, Emitech Ltd., Ashford, Kent, UK) for 30 s and 80 mA prior to imaging.

C, H, N, O and S content of the samples was determined using elemental analysis (EA 1108 CHNS–O, Carlo Erba Instruments).

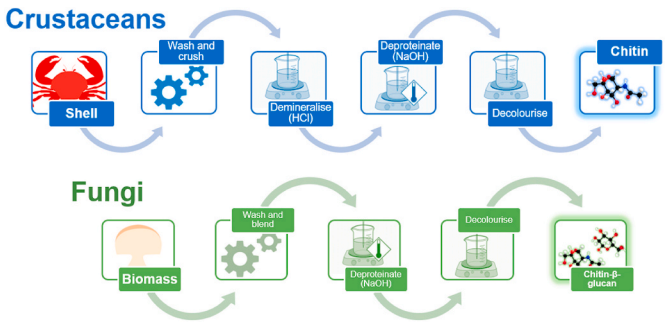

Fig. 1. Chitin extraction process for crustacean- and fungi-derived chitin, comprising mechanical (crushing or blending) and chemical (demineralisation, deproteination and decolourisation) treatments. Adapted from Jones et al. [12].

Carbohydrate analysis was performed using high performance anion exchange chromatography (HPEAC). Initially, 300 mg of freeze-dried sample was dispersed in 3 mL of 72% H_2SO_4 at 30 °C for 60 min, subsequently diluted with water (4%) and placed in an autoclave at 121 °C for 60 min. The acid hydrolysate was analysed using HPAEC (Dionex ICS3000 chromatograph equipped with a CarboPac PA20 column). Prior to HPAEC analysis, sugar recovery standards were prepared and pre-treated at identical hydrolysis conditions in order to analyse their recovery throughout the procedure.

2.7. Analysis of the molecular structure of (composite) nanopapers

IR spectra were recorded using a Spectrum One FTIR-spectrometer (PerkinElmer, Massachusetts, USA). A total of 16 scans were measured and averaged to produce each spectrum. Spectra were recorded across the range of 4000-600 cm^{-1}. Variations in the penetration depth of infrared radiation were corrected using built-in software and the baseline based on Duarte, Ferreira, Marvao and Rocha [18].

XRD was measured using an X-ray diffractometer (PANanalytical X'pert Pro, PANanalytical Ltd., Cambridge, UK) equipped with a 1.54 Å Cu K_α X-ray source. Samples (~10 mm × 10 mm) were rotated at 16 rpm to avoid possible orientation effects and irradiated on a zero-background silicon plate. All measurements were recorded in the range $5° \leq 2\theta \leq 40°$ with a step size of 0.02° and scan speed of 30 s. The crystallinity index (CI%) of all samples was calculated based on the area under the diffraction pattern [19,20], instead of the more common peak height method. The deconvolution method of Goodrich and Winter [21] was applied to the data. Briefly, the baseline corrected diffraction data was smoothed by applying a Savitsky-Golay filter using a second-order polynomial function with 10 points and deconvoluted using a Gaussian function. The total area under the crystalline diffraction peaks was then divided by the total area under the curve for the range $5° \leq 2\theta \leq 30°$. Crystallite size L_{020} was calculated using Scherrer's equation [22] (equation (1)), based on Bragg's angle θ [°], full width at half maximum of the 020 reflection β [π^c] and the wavelength of the X-ray source λ [Å]:

$$L_{020} = \frac{0.93 \times \lambda}{\beta \times \cos\theta} \quad (1)$$

2.8. Physical and mechanical properties of (composite) nanopapers

Nanopapers were cut into dog bone shaped specimens (shape according to ASTM D638-14) using a Zwick ZCP 020 Manual Cutting Press. Specimens had a parallel width of 2 mm and an overall length of 35 mm. The thickness of each specimen was determined using a handheld microscope on polished epoxy embedded samples, calibrated using 100 × 0.01 mm microscope graticule (Graticules Ltd., Tonbridge, Kent, UK). Tensile tests were performed using a TST350 tensile tester (TST350, Linkam Scientific Instruments, Surrey, UK) fitted with a 200 N load cell. Specimens were fixed between metal clamps using testing cards to avoid perforation of the clamped sample ends. Testing velocity was 1 mm/min with gauge length set to 10 mm. The elastic modulus (E) was analysed from the linear elastic region as a secant between strength values separated by 0.2% strain. The tensile strength σ was calculated from maximum load and specimen cross-sectional area. The machine compliance, 6.38×10^{-3} mm/N, was determined in accordance with ASTM C1557-14 and accounted for in all tests.

The skeletal density ρ_s of the nanopapers was analysed using a helium gas displacement pycnometer (AccuPyc II 1340, Micromeritics, Aachen, Germany) using a 1 cm^3 sample chamber. A total of 10 replicate measurements were performed at 23 ± 1 °C and averaged.

Porosity was measured using mercury intrusion porosimetry (AutoPore IV 9500, Micromeritics). Sample envelope density ρ_e was measured at 0.002 MPa, with pores larger than 150 μm filled by mercury. True sample porosity φ was then calculated based on equation (2):

$$\varphi(\%) = \left(1 - \frac{\rho_e}{\rho_s}\right) \times 100 \quad (2)$$

2.9. Surface energy analysis of (composite) nanopapers

Static water contact angles θ were measured over 60s on 10 μL droplets deposited onto nanopaper surfaces using the sessile drop method (DSA 10 MK2, Krüss, Hamburg, Germany). The experiment was conducted at room temperature and at least five contact angles were measured using a tangent-1 fit method.

Moisture sorption behaviour was investigated using dynamic vapour sorption (DVS Intrinsic, Surface Measurement Systems, London, UK). Samples were exposed to 0%, 50% and 90% RH, for 12 h periods cycling back to 0% RH after each condition to equilibrate for the same period. All measurements were run at 25 °C and the change in mass resulting from moisture sorption measured as a function of time.

Surface free energy was measured by inverse gas chromatography (iGC) (SEA, Surface Measurement Systems, UK). The surface energy of nanopapers was determined at 30 °C and 0% RH. Nanopaper samples were cut and inserted into a pre-silanized measurement column. A series of n-alkanes (hexane, heptane, octane, nonane, decane) were used for the determination of the dispersive component of the surface energy γ^d. The acid-base components of the surface tension γ^{ab} were determined using the polar probes dichloromethane and ethyl acetate. The vapours were passed over the nanopaper samples and the retention times and volumes recorded. All chromatogram peaks were defined using first statistical moment at the peak's centre of mass (Peak COM) and the net retention volumes calculated using the Schultz method [23].

ζ-potential of nanopapers was determined as a function of pH using an electrokinetic analyser (Anton Paar SurPASS, Graz, Austria). The ζ-potential was measured in an adjustable gap cell (100 μm), with electrolyte solution (1 mM KCl) pumped through the cell at pressures steadily increased to 300 mbar. The pH was controlled by titrating 0.1 M KOH and 0.1 M HCl into the electrolyte solution and the ζ-potential determined from the streaming potential.

3. Results and discussion

3.1. Chemical and elemental analysis of the polymer extract

Extracts of both *A. bisporus* and *D. confragosa* fungal fruiting bodies contained significantly less N (3.4 wt.% and 0.2 wt.%, respectively) and glucosamine (56.9 wt.% and 1.1 wt.%, respectively) than *C. pagurus* crustacean-derived chitin (6.4 wt.% N and 84.5 wt.% glucosamine), which closely matched in composition that of the commercial chitin reference (6.5 wt.%, N and 85.9 wt.% glucosamine) (Tables 1 and 2). This indicated a significantly lower chitin content in the fungal extract than in the commercial and crustacean-derived reference materials and can be attributed to the high glucan content of fungal biomass. Fungal chitin is covalently decorated with β-glucan, as indicated by the higher O content (46.7–50.6 wt.% compared to 39.6 wt.% for commercial chitin) associated with the large number of hydroxyl groups in β-glucan. The

Table 1
Elemental composition and dry weight yield of a commercial chitin reference, crab crustacean chitin (*C. pagurus*) and fungal extracts derived from *A. bisporus* and *D. confragosa* fruiting bodies. All standard deviations are <0.5 wt.%.

Sample	Elemental composition (wt.% of total mass)					Yield
	C	H	N	O	S	(%)
Commercial chitin (reference)	44.6	7.3	6.5	39.6	<0.02	–
C. pagurus (crab shell)	43.8	7.2	6.4	39.7	<0.02	9.7
A. bisporus (common mushroom)	42.8	7.1	3.4	46.7	<0.02	15.0
D. confragosa (bracket fungus)	43.3	6.5	0.2	50.6	<0.02	69.8

Table 2
Sugar composition based on fraction of total sugars present in a commercial chitin reference, crab crustacean chitin (*C. pagurus*) and fungal polymer extracts derived from *A. bisporus* and *D. confragosa* fruiting bodies.

Sample	Sugar[a] composition (wt.% of total sugars)		
	Glucosamine	Glucose	Mannose
Commercial chitin (reference)	85.9	0.0	14.1
C. pagurus (crab shell)	84.5	0.0	15.5
A. bisporus (common mushroom)	56.9	42.6	0.0
D. confragosa (bracket fungus)	1.1	98.9	0.0

[a] Galactose, xylose, arabinose, rhamnose were not detected in the samples.

high glucan content of the fungi-derived samples was also demonstrated by sugar analysis, which found *A. bisporus* and *D. confragosa* extracts to have glucose contents of 42.6 wt.% and 98.9 wt.%, respectively, compared with the negligible glucose contents of the commercial and crustacean-derived references. *A. bisporus* fruiting body extract had an almost 1.4:1 ratio of chitin to glucan while the *D. confragosa* extracts had a negligible chitin content, representing almost exclusively glucan-rich polysaccharides. Both elemental and sugar analysis of the *D. confragosa* extract resemble literature values for the yeast cell wall polysaccharide (1 → 3)/(1 → 6)-β-D-glucan [24]. The origin of the mannose content in the *C. pagurus* crustacean derived chitin is unclear but is mirrored in the commercial chitin reference.

ATR-FTIR spectra (Fig. S1a Supplementary Data) showed the presence of chitin in the *A. bisporus* fruiting body extracts and almost complete lack thereof in the *D. confragosa* samples. XRD diffractograms (Fig. S1b Supplementary Data) also indicated that *A. bisporus* fruiting bodies exhibited low crystallinity and that a considerable amount of amorphous material was present, likely attributable to the large quantity of β-glucan. The presence of amorphous glucan was also probably responsible for the smaller crystallite size in *A. bisporus* fungal samples (40.6 Å) compared to the commercial (66.9 Å) and *C. pagurus* crustacean chitin (63.8 Å) reference samples (Table 3). *D. confragosa* fungal derived nanopapers did not exhibit chitin-associated peaks, instead resembling linear (1 → 3)-β-glucans or branched (1 → 3)/(1 → 6)-β-glucans [24–27].

Nanopapers produced from the extracts of *A. bisporus* and *D. confragosa* fruiting bodies exhibited low isoelectric points (i.e.p) (3.0 and 2.6, respectively) and ζ-potential plateau values ($\zeta_{plateau}$) at high pH associated with full deprotonation of all dissociable functional groups (Fig. 2). This indicated an acidic surface character, originating from the carboxyl groups in the glucan chains associated with fungal chitin. The difference in disassociation energy between the free amino groups of chitin and glucan's acid surface groups also resulted in a pronounced minimum in the ζ-potential of fungal samples with a high chitin content, such as *A. bisporus*, which grew less pronounced with reducing chitin content and was absent altogether in samples comprising almost entirely β-glucan, such as *D. confragosa*. Fungal nanopapers were more acidic than a cellulose-based filter paper reference (i.e.p. = 3.7), indicating the presence of some uronic acid groups. Conversely, *C. pagurus* crustacean derived chitin nanopapers exhibited a sigmoidal ζ = f(pH) curve, which indicated an amphoteric surface character. Protonation of chitin's free amino group (degree of deacetylation, DD = 12%) at low pH imparted a positive charge on the surface of these nanopapers and hence positive

Table 3
Crystallinity index CI [%] based on the area under the diffraction peaks deconvoluted according to Goodrich and Winter [21] and crystallite size L_{020} [Å] based on Scherrer's equation [22].

Sample	CI (%)	L_{020} (Å)
Commercial chitin (reference)	76	67
C. pagurus (crab shell)	86	64
A. bisporus (common mushroom)	66	41

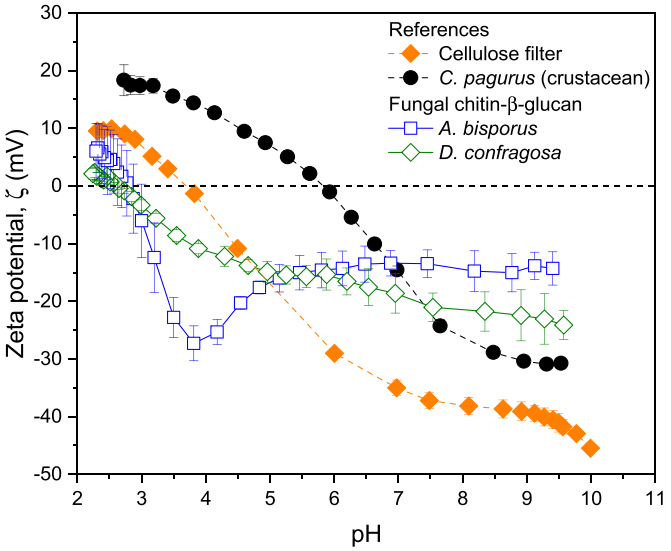

Fig. 2. ζ-potential measured in 1 mM KCl as a function of pH for *A. bisporus* (blue) and *D. confragosa* (green) nanopapers, compared to *C. pagurus* (crustacean) nanopapers (black dotted) and cellulose filter paper (orange dotted). (For interpretation of the references to colour in this figure legend, the reader is referred to the Web version of this article.)

ζ-potential, in the broad acidic region. Lacking the glucan content of fungal chitin, the basic amino groups of the *C. pagurus* crustacean chitin were also more in balance with the acidic groups in the chitin chain, resulting in an i.e.p at pH of 5.8. This i.e.p. indicated that the DD of the crustacean-derived nanopapers was significant, since pure chitin typically has an i.e.p of 3.5 [28], with the i.e.p. of chitosan ranging from 7 to 9 [29,30].

3.2. Physical and mechanical properties of the nanopapers

All papers produced from *A. bisporus* and *D. confragosa* fruiting bodies were brown in colour. *D. confragosa* samples were opaque, while *A. bisporus* nanopapers were quite transparent (Fig. 3). These differences in transparency could be attributed to differences in nanoscale surface morphology. *A. bisporus* nanopapers comprised dense, randomly orientated nanofibre networks, with fibrils ranging from 10 to 20 nm in diameter (Fig. 4a) similar to literature [31]. Conversely, *D. confragosa* papers comprised much larger, uniform width microfibres, with diameters ranging from 1 to 2 μm (Fig. 4b).

Variations in fibre morphology enabled the production of composite nanopapers with tuneable transparency, physical and tensile properties, by varying the content of each respective fungal fruiting body extract. The nanoscale surface morphologies of composite nanopapers

Fig. 3. Visual representation of *D. confragosa* (opaque) papers, *A. bisporus* nanopapers (transparent) and composite nanopapers containing 75:25, 50:50 and 25:75 wt.% *D. confragosa* to *A. bisporus* extracts compared to *C. pagurus* (crab) crustacean chitin reference nanopapers. Transparency is achieved with an *A. bisporus* loading as low as 25 wt.%.

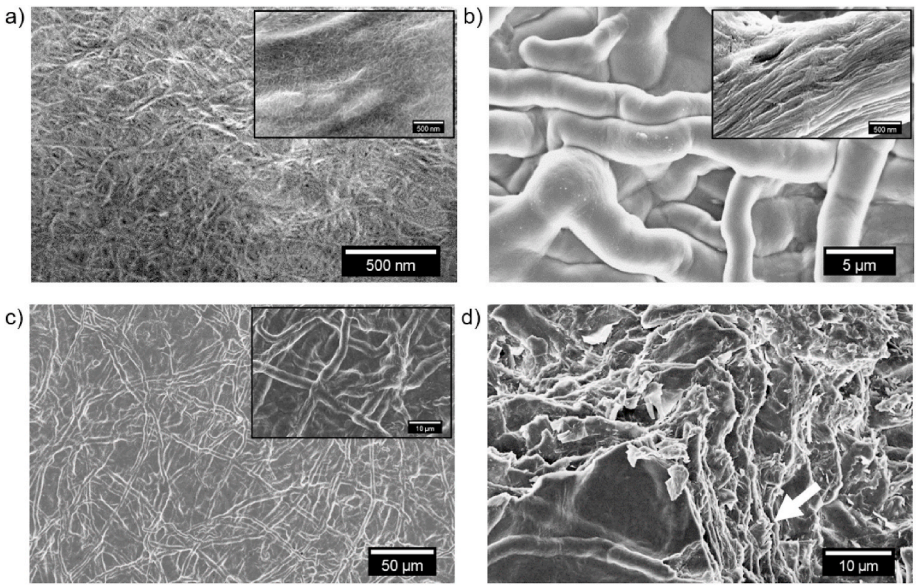

Fig. 4. SEM micrographs showing the surface morphology of (a) *A. bisporus* nanopapers, (b) *D. confragosa* papers and the (c) surface morphology nanopaper and (d) fracture surface of 50 wt.% *A. bisporus* + 50 wt.% *D. confragosa* composite nanopapers. The fracture surface of the composite nanopapers exhibited a combination of brittle behaviour resulting from the *A. bisporus* nanofibres and fibre pull-out associated with the ductile behaviour of *D. confragosa* microfibres (indicated by arrow). Insets provide higher magnification micrographs of nanopaper surface morphologies.

comprising each fruiting body extract in a 1:1 ratio clearly showed the coating of the *D. confragosa* microfibres with *A. bisporus* nanofibres (Fig. 4c), which impart a combination of ductile tensile properties due to microfibre pull-out and brittle characteristics derived from the nanofibres (Fig. 4d).

The effect of the different fibre diameters and failure mechanisms of the *A. bisporus* and *D. confragosa* nanopapers was apparent in their tensile properties, with smaller diameter fibers forming stronger networks with a smaller number of defects. *D. confragosa* papers had a tensile strength of 65.3 MPa, elastic modus of 1.2 GPa and 13.2% elongation at break, making them ductile and tough. Conversely, *A. bisporus* nanopapers were much stronger (204.4 MPa tensile strength) and stiffer (6.9 GPa elastic modulus) but were also more brittle, with less than half the elongation at break (5.3%) (Fig. 5). Notably, both fungal papers had comparable or higher tensile strengths than *C. pagurus* crustacean chitin nanopapers (65–204 MPa compared to 70 MPa) and

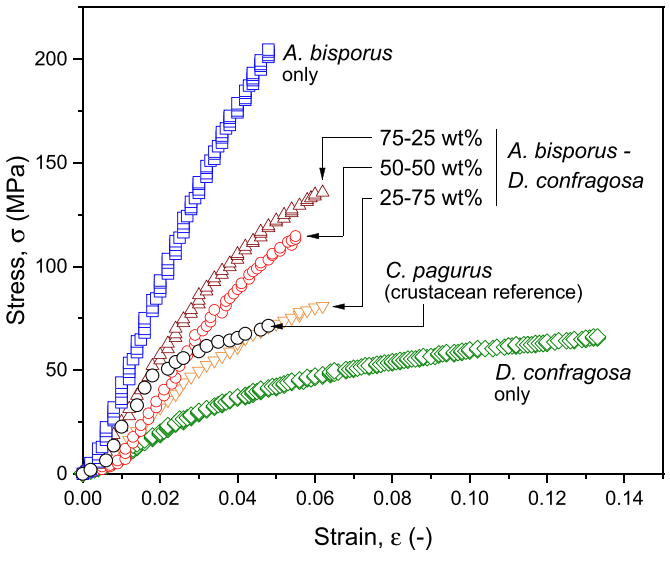

Fig. 5. Tensile stress-strain curves for *A. bisporus* (blue), *D. confragosa* (green), composite (25:75, orange, 50:50, red and 75:25 wt.%, brown) nanopapers and a *C. pagurus* crustacean reference (black). (For interpretation of the references to colour in this figure legend, the reader is referred to the Web version of this article.)

A. bisporus samples had a similar elongation at break (5.3% compared to 6.2%) despite being almost 3 times stronger. These improved tensile properties compared to both our crustacean-derived samples and values for crustacean-derived films with a similar fibre (10–20 nm) diameter reported in the literature [32,33], could result from the milder alkaline treatment used to process fungal fruiting bodies, compared to the harsher acid treatment necessary to extract chitin from crustacean sources and the presence of amorphous glucan in fungi, acting as matrix in the fibre network thus mitigating the brittleness of chitin. Variations in *A. bisporus* and *D. confragosa* extract content in 25 wt.% increments allowed the tensile strength, elastic modulus, elongation at break and work of fracture of composite nanopapers to be tuned between the properties exhibited by the pure *A. bisporus* and *D. confragosa* nanopapers as desired. These variations were also associated with small differences in density and porosity (Table 4).

3.3. Surface properties of the nanopapers

A. bisporus and *D. confragosa* fungal fruiting body extract derived (nano)papers had higher static water contact angles θ (65.6° and 54.5°, respectively) than crustacean derived *C. pagurus* nanopapers (24.2°) (Fig. 6) similar to those reported in literature [34]. These significant differences in θ were stable over 60 s (Fig. S2 Supplementary Data) and supported by iGC data, with lower total surface energies γ_t recorded for fungi-than crustacean-derived nanopapers (52.5 mJ/m^2 and 55.7 mJ/m^2 for *A. bisporus* and *D. confragosa*, respectively, compared to 72.5 mJ/m^2 for *C. pagurus* crustacean derived samples) (Table 5). Water contact angles as high as 50–55° having been recorded in the literature for similar films prepared under higher pressure [35,36]. Subsequently, the water contact angle of *D. confragosa* was comparable with literature values for crustacean chitin and significantly higher than those for cellulose [37], while *A. bisporus* samples were undoubtedly more hydrophobic than both of these other natural materials.

D. congragosa and *A. bisporus* fungi-derived nanopapers had slightly higher moisture contents (2.9 wt.% and 4.2 wt.%, respectively) than the *C. pagurus* crustacean reference (2.8 wt.%) at ambient conditions. However, *A. bisporus* fungi-derived nanopapers had similar moisture uptake characteristics to *C. pagurus* samples at 50% RH (~8 wt.%), only absorbing more water than the crustacean reference at 90% RH (~33 wt.% compared to ~21 wt.%) (Fig. S3 Supplementary Data). *D. confragosa* exhibited the highest moisture uptake at 50% RH (~11 wt.%) but had similar moisture uptake characteristics to *A. bisporus*

Table 4
Composition, envelope ρ_e and skeletal ρ_s density [g/m^3], porosity φ [%], ultimate tensile strength σ_{UTS} [MPa], elastic modulus E [MPa], strain to failure ε_f [%] and work of fracture W_F [MJ/m^3] for *A. bisporus*, *D. confragosa*, composite (25:75, 50:50, 75:25 wt.%) nanopapers and a *C. pagurus* (crab shell) crustacean chitin nanopaper reference.

Composition (wt.%)		ρ_e	ρ_s	φ	Tensile properties			
A. bisporus	*D. confragosa*	(g/cm^3)		(%)	σ_{UTS} (MPa)	E (GPa)	ε_f (%)	W_F (MJ/m^3)
C. pagurus (crab shell)		0.46	1.40	67.3	69.5 ± 4.6	2.7 ± 0.5	6.2 ± 0.7	2.7 ± 0.4
0	100	0.69	1.54	55.0	65.3 ± 0.8	1.2 ± 0.1	13.2 ± 1.2	5.8 ± 0.5
25	75	0.77	1.51	49.0	82.7 ± 4.2	2.1 ± 0.4	6.3 ± 0.5	3.0 ± 0.4
50	50	0.77	1.49	48.6	114.8 ± 4.2	3.0 ± 0.5	5.7 ± 0.3	3.5 ± 0.3
75	25	0.74	1.48	49.8	136.0 ± 6.0	3.7 ± 0.4	6.1 ± 0.2	4.5 ± 0.3
100	0	0.60	1.47	59.0	204.4 ± 4.0	6.9 ± 1.2	5.3 ± 0.4	5.3 ± 0.5

nanopapers at 90% RH (~31 wt.%). The lower wettability of *A. bisporus* compared to *D. confragosa* and crustacean-derived samples can be attributed to the higher degree of acetylation resulting in a lower surface polarity of the nanopapers produced from more mildly treated fungal chitin fibrils compared to crustacean chitin and its lower glucan content compared to *D. confragosa* (Table 2). The lower acid-base surface energy component γ^{ab}, as determined by iGC, of the *A. bisporus* nanopaper compared to the *C. pagurus* crustacean-derived sample (6.2 mJ/m^2 compared with 18.1 mJ/m^2, respectively) (Fig. 7) resulted from the lower number of polar amide groups in the chitin-β-glucan fungal polymer due to the glucan content. The hydroxyl groups of β-glucan are less polar than chitin's amide groups, giving the fungal samples lower surface polarity and a more hydrophobic character than crustacean chitin.

The comparatively high hydrophobicity of *A. bisporus* fungal extract could potentially be exploited as a coating agent for otherwise very hydrophilic materials, such as cellulose, with even thin coatings (0.8% w/v) preventing water absorption through blotting paper (Fig. 6d). Alkaline treated fungal chitin extracts derived from mycelium (vegetative growth of filamentous fungi) grown on agricultural by-products, such as blackstrap molasses, are even more hydrophobic (advancing water contact angles up to ~106°) due to impurities they contain, such as lipid residues [38], and one could build upon this principle to achieve even more hydrophobic fungal chitin coatings.

4. Conclusion

Fungal chitin offers a cheap, renewable, easily isolated and abundant alternative to crustacean chitin, with the native nanocomposite architecture of chitin-β-glucan that fungi contain providing additional remarkable opportunities for tuning the mechanical and surface properties of fungi-derived materials. This chitin-β-glucan complex can be readily extracted from fungi using a mild alkaline process, as opposed to the harsh demineralisation required for crustacean chitin and hot pressed into engineered composite nanopapers. Common white button mushrooms (*A. bisporus*) have almost proportional contents of chitin and β-glucan, which acts as matrix in the chitin fibre network, with a nanofibrous architecture resulting in very high tensile strengths, far outperforming crustacean-derived chitin nanopapers. The properties of these nanopapers can be tuned in a controlled fashion by increasing their β-glucan content through the addition of extract from tree bracket fungi (*D. confragosa*), which comprise almost entirely β-glucan. Composite nanopaper tensile performance can be tuned from more brittle, high tensile strength nanofibrous materials to very tough and elastomeric rubber-like materials exhibiting significant microfibre pull-out at failure. These remarkable and controllable characteristics make fungi-derived materials highly versatile for a wide range of applications, including coatings, membranes, packaging and paper.

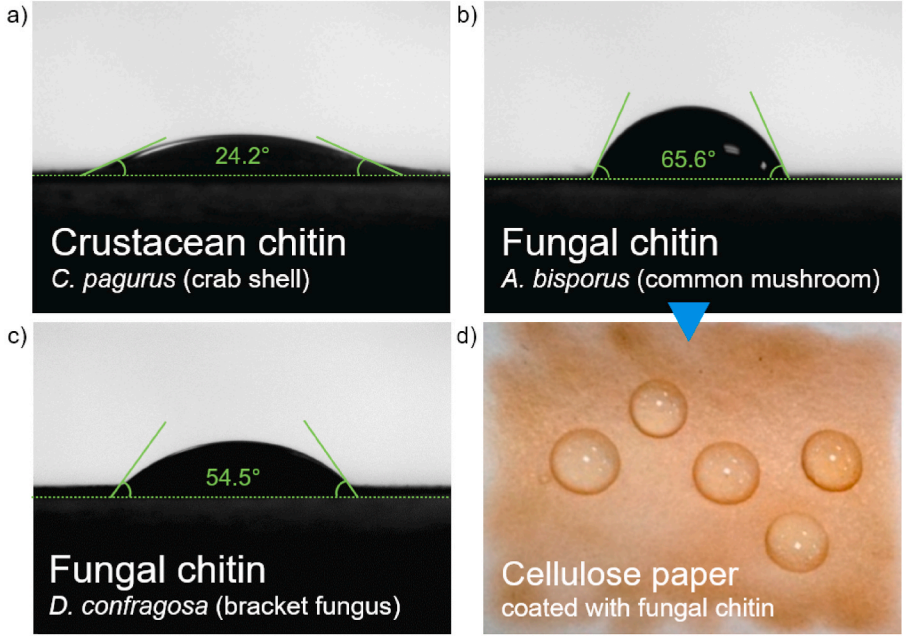

Fig. 6. Static water contact angles for droplets on (a) *C. pagurus* (crab shell) crustacean chitin reference, (b) *A. bisporus* (common mushroom) and (c) *D. confragosa* (bracket fungus) fungal chitin nanopapers. The hydrophobic effect that a 0.8 w/v *A. bisporus* fungal chitin coating has on cellulose paper is also depicted (d).

Table 5
Dispersive γ^d, acid-base γ^{ab} surface energy components and total surface energy γ^t [mJ/m^2] at n/n$_m$ = 0.01 for *A. bisporus*, *D. confragosa* fungal chitin nanopapers and a *C. pagurus* (crab shell) crustacean reference nanopaper.

Sample	Surface energy component (mJ/m^2)		
	γ^d	γ^{ab}	γ^t
C. pagurus (crab shell)	54.4	18.1	72.5
A. bisporus (common mushroom)	46.3	6.2	52.5
D. confragosa (bracket fungus)	49.3	6.4	55.7

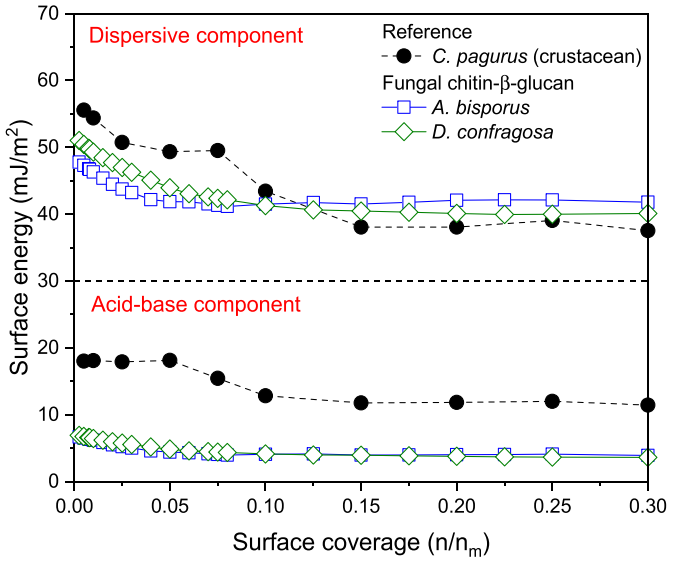

Fig. 7. Dispersive (γ^d) and acid-base (γ^{ab}) surface energy components [mJ/m^2] determined by iGC as a function of surface coverage for *A. bisporus* (blue), *D. confragosa* (green) fungal chitin nanopapers and a *C. pagurus* crustacean reference (black). (For interpretation of the references to colour in this figure legend, the reader is referred to the Web version of this article.)

Declaration of competing interest

The authors declare that they have no known competing financial interests or personal relationships that could have appeared to influence the work reported in this paper.

CRediT authorship contribution statement

Wan M.F.W. Nawawi: Conceptualization, Formal analysis, Writing - original draft, Writing - review & editing. **Mitchell P. Jones:** Writing - original draft, Writing - review & editing. **Eero Kontturi:** Formal analysis, Writing - review & editing. **Andreas Mautner:** Supervision, Writing - review & editing. **Alexander Bismarck:** Conceptualization, Writing - review & editing, Supervision, Writing - review & editing.

Acknowledgments

WMFWN acknowledges the financial support of the International Islamic University Malaysia and Ministry of Higher Education (Malaysia). Funding by the University of Vienna for AM is also acknowledged. The authors thank Johannes Theiner (Mikroanalytisches Laboratorium, Faculty of Chemistry, University of Vienna) for elemental analysis. E.K. is grateful for the support by the FinnCERES Materials Bioeconomy Ecosystem.

Appendix A. Supplementary data

Supplementary data to this article can be found online at https://doi.org/10.1016/j.compscitech.2020.108327.

References

[1] G. Holt, G. Mcintyre, D. Flagg, E. Bayer, J. Wanjura, M. Pelletier, Fungal mycelium and cotton plant materials in the manufacture of biodegradable molded packaging material: evaluation study of select blends of cotton byproducts, J. Biobased Mater. Bioenergy 6 (4) (2012) 431–439.
[2] M. Jones, T. Huynh, C. Dekiwadia, F. Daver, S. John, Mycelium composites: a review of engineering characteristics and growth kinetics, J. Bionanoscience 11 (4) (2017) 241–257.
[3] W. Nawawi, M. Jones, R.J. Murphy, K.-Y. Lee, E. Kontturi, A. Bismarck, Nanomaterials derived from fungal sources - is it the new hype? Biomacromolecules 21 (1) (2020) 30–55.
[4] M. Jones, A. Mautner, S. Luenco, A. Bismarck, S. John, Engineered mycelium composite construction materials from fungal biorefineries: a critical review, Mater. Des. (2020) 108397.
[5] M. Rinaudo, Chitin and chitosan—general properties and applications, ChemInform 38 (7) (2007) 603–632.
[6] Y. Bamba, Y. Ogawa, T. Saito, L.A. Berglund, A. Isogai, Estimating the strength of single chitin nanofibrils via sonication-induced fragmentation, Biomacromolecules 18 (12) (2017) 4405–4410.
[7] J. Webster, R. Weber, Introduction to Fungi, Cambridge University Press, Cambrige, U.K., 2007.
[8] S. Ifuku, Chitin and chitosan nanofibers: preparation and chemical modifications, Molecules 19 (11) (2014) 18367–18380.
[9] F. Di Mario, P. Rapana, U. Tomati, E. Galli, Chitin and chitosan from basidiomycetes, Int. J. Biol. Macromol. 43 (1) (2008) 8–12.
[10] A. Hassainia, H. Satha, S. Boufi, Chitin from agaricus bisporus: extraction and characterization, Int. J. Biol. Macromol. 117 (1) (2018) 1334–1342.
[11] R.A. Muzzarelli, Chitin nanostructures in living organisms, chitin, Springer, Berlin, Germany, 2011, pp. 1–34.
[12] M. Jones, M. Kujundzic, S. John, A. Bismarck, Crab vs. mushroom: a review of crustacean and fungal chitin in wound treatment, Mar. Drugs 18 (2020) 64.
[13] J. Sietsma, J. Wessels, Chemical analysis of the hyphal walls of Schizophyllum commune, Biochim. Biophys. Acta Gen. Subj. 496 (1) (1977) 225–239.
[14] W. Nawawi, K.-Y. Lee, E. Kontturi, R. Murphy, A. Bismarck, Chitin nanopaper from mushroom extract: natural composite of nanofibres and glucan from a single biobased source, ACS Sustain. Chem. Eng. 7 (7) (2019) 6492–6496.
[15] M. Rice, Get an old blender and make your own deckle and mould, Mushroom: The Journal of Wild Mushrooming 10 (36) (1992) 22–26.
[16] M. Rice, A kitchen-variety approach to fine paper from mushrooms, Mushroom, The Journal of Wild Mushrooming 10 (34) (1991) 21–22.
[17] I. Younes, M. Rinaudo, Chitin and chitosan preparation from marine sources. Structure, properties and applications, Mar. Drugs 13 (3) (2015) 1133–1174.
[18] M. Duarte, M. Ferreira, M. Marvao, J. Rocha, An optimised method to determine the degree of acetylation of chitin and chitosan by FTIR spectroscopy, Int. J. Biol. Macromol. 31 (1-3) (2002) 1–8.
[19] B. Focher, P. Beltrame, A. Naggi, G. Torri, Alkaline N-deacetylation of chitin enhanced by flash treatments. Reaction kinetics and structure modifications, Carbohydr. Polym. 12 (4) (1990) 405–418.
[20] Y. Zhang, C. Xue, Y. Xue, R. Gao, X. Zhang, Determination of the degree of deacetylation of chitin and chitosan by X-ray powder diffraction, Carbohydr. Res. 340 (11) (2005) 1914–1917.
[21] J.D. Goodrich, W.T. Winter, α-Chitin nanocrystals prepared from shrimp shells and their specific surface area measurement, Biomacromolecules 8 (1) (2007) 252–257.
[22] A. Patterson, The Scherrer formula for X-ray particle size determination, Phys. Rev. 56 (10) (1939) 978.
[23] J.a. Schultz, L. Lavielle, C. Martin, The role of the interface in carbon fibre-epoxy composites, J. Adhes. 23 (1) (1987) 45–60.
[24] M. Novák, A. Synytsya, O. Gedeon, P. Slepička, V. Procházka, A. Synytsya, J. Blahovec, A. Hejlová, J. Čopíková, Yeast β (1-3) , (1-6) -d-glucan films: preparation and characterization of some structural and physical properties, Carbohydr. Polym. 87 (4) (2012) 2496–2504.
[25] J. Jelsma, D.R. Kreger, Observations on the cell-wall compositions of the bracket fungi Laetiporus sulphureus and Piptoporus betulinus, Arch. Microbiol. 119 (3) (1978) 249–255.
[26] T. Harada, K. Okuyama, A. Konno, A. Koreeda, A. Harada, Effect of heating on formation of curdlan gels, Carbohydr. Polym. 24 (2) (1994) 101–106.
[27] N. Tamura, M. Wada, A. Isogai, TEMPO-mediated oxidation of (1→ 3)-β-d-glucans, Carbohydr. Polym. 77 (2) (2009) 300–305.
[28] M. Wysokowski, Ł. Klapiszewski, D. Moszyński, P. Bartczak, T. Szatkowski, I. Majchrzak, K. Siwińska-Stefańska, V.V. Bazhenov, T. Jesionowski, Modification of chitin with kraft lignin and development of new biosorbents for removal of cadmium(II) and nickel(II) ions, Mar. Drugs 12 (4) (2014) 2245–2268.
[29] M. Gouda, U. Elayaan, M.M. Youssef, Synthesis and biological activity of drug delivery system based on chitosan nanocapsules, Adv. Nanoparticles 3 (4) (2014) 148.
[30] S. Swain, R. Dey, D.M. Islam, R. Patel, U. Jha, T. Patnaik, C. Airoldi, Removal of fluoride from aqueous solution using aluminum-impregnated chitosan biopolymer, Separ. Sci. Technol. 44 (9) (2009) 2096–2116.
[31] S. Ifuku, R. Nomura, M. Morimoto, H. Saimoto, Preparation of chitin nanofibers from mushrooms, Materials 4 (8) (2011) 1417–1425.

[32] S. Ifuku, S. Morooka, A.N. Nakagaito, M. Morimoto, H. Saimoto, Preparation and characterization of optically transparent chitin nanofiber/(meth) acrylic resin composites, Green Chem. 13 (7) (2011) 1708–1711.
[33] N. Ezekiel Mushi, N. Butchosa, Q. Zhou, L.A. Berglund, Nanopaper membranes from chitin–protein composite nanofibers—structure and mechanical properties, J. Appl. Polym. Sci. 131 (7) (2014).
[34] W.M.F.W. Nawawi, K.-Y. Lee, E. Kontturi, A. Bismarck, A. Mautner, Surface properties of chitin-glucan nanopapers from Agaricus bisporus, Int. J. Biol. Macromol. 148 (2020) 677–687.
[35] K. Gopalan Nair, A. Dufresne, A. Gandini, M.N. Belgacem, Crab shell chitin whiskers reinforced natural rubber nanocomposites. 3. Effect of chemical modification of chitin whiskers, Biomacromolecules 4 (6) (2003) 1835–1842.
[36] M.I. Shams, S. Ifuku, M. Nogi, T. Oku, H. Yano, Fabrication of optically transparent chitin nanocomposites, Appl. Phys. A 102 (2) (2011) 325–331.
[37] G. Siqueira, J. Bras, A. Dufresne, New process of chemical grafting of cellulose nanoparticles with a long chain isocyanate, Langmuir 26 (1) (2010) 402–411.
[38] M. Jones, K. Weiland, M. Kujundzic, J. Theiner, H. Kahlig, E. Kontturi, S. John, A. Bismarck, A. Mautner, Waste-derived low-cost mycelium nanopapers with tunable mechanical and surface properties, Biomacromolecules 20 (9) (2019) 3513–3523.